"Abrupt climate variability during the last glacial period and Termination"

Spatial Gradient and Temporal Variations in $^{17}O_{excess}$

Spruce Schoenemann, Qinghua Ding, Eric Steig,
Andrew Schauer, Vasileios Gkinis, & Bradley Markle
University of Washington

Introduction

Recent development of techniques to measure the $^{17}O/^{16}O$ ratio precisely has allowed $^{17}O_{excess}$ to be added to the ice-core isotope toolbox. In combination with traditional $\delta^{18}O$ and dexcess measurements, $^{17}O_{excess}$ provides valuable new information on the evaporative conditions of the oceanic moisture sources and may be used to disentangle the competing effects of fractionation at the source, during transport, and in the formation and deposition of precipitation. We measured $\delta^{17}O$ and $\delta^{18}O$ from a number of Antarctic ice cores (West Antarctic Ice Sheet Divide, Siple Dome, Taylor Dome), and present $^{17}O_{excess}$ values for the modern, Holocene, and glacial periods using traditional fluorination and IRMS techniques. These results, combined with results from Talos Dome, Dome C, and Vostok (Landais et al. [2008]; Winkler et al. [2011]), provide the most complete spatial and temporal view of Antarctic $^{17}O_{excess}$ to date.

Location of WAIS Divide, Taylor Dome, Siple Dome and other East Antarctic Ice Cores

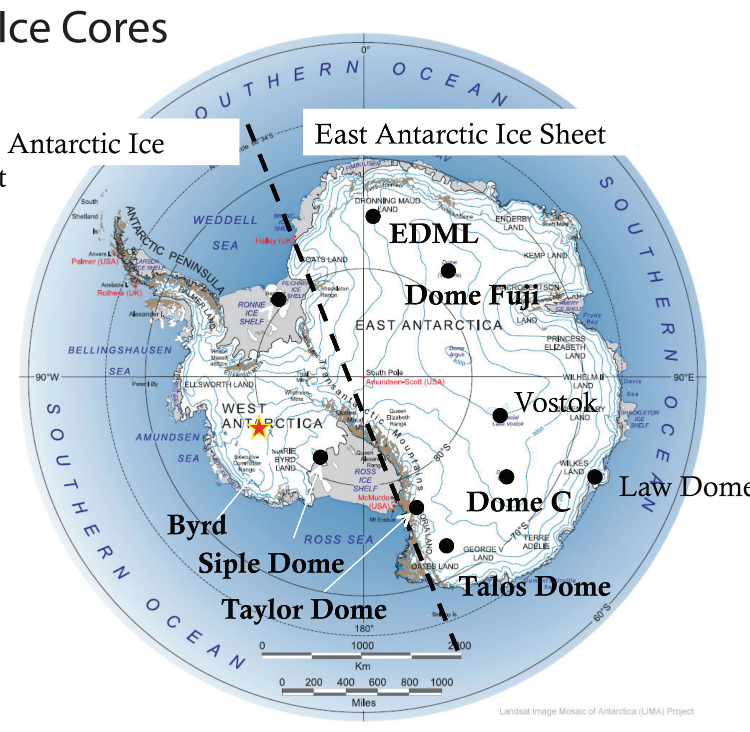

$^{17}O_{excess}$ Measurements from LGM to Holocene:

WAIS Divide

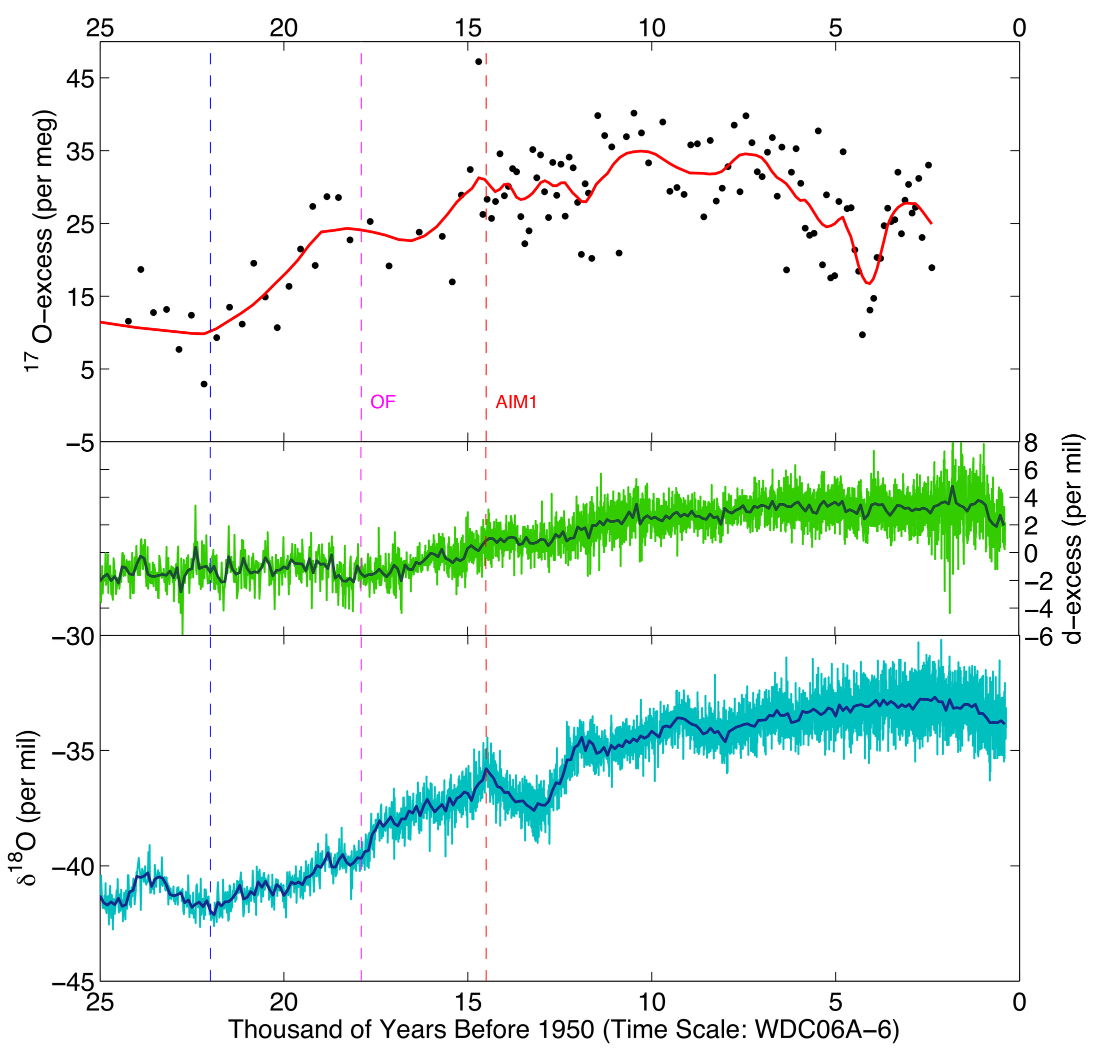

Figure 1. Timeseries of $^{17}O_{excess\,VSMOW\text{-}SLAP}$ (top), deuterium excess (middle), and $\delta^{18}O$ (bottom) of the WAIS Divide (WD) ice core record from 25ka to 0ka. The glacial (24-19.5ka) to Early Holocene (11-7.5ka) transition shows a significant 20 per meg (p<0.005) increase in $^{17}O_{excess}$. Blue dashed line indicates early deglacial warming at ~22ka, magenta dashed line indicates the Old Faithful (OF) stratigraphic layer marking abrupt $\delta^{18}O$ increase (see Fudge et al. Poster), and red dashed line indicates AIM1 at 14.5ka.

Siple Dome

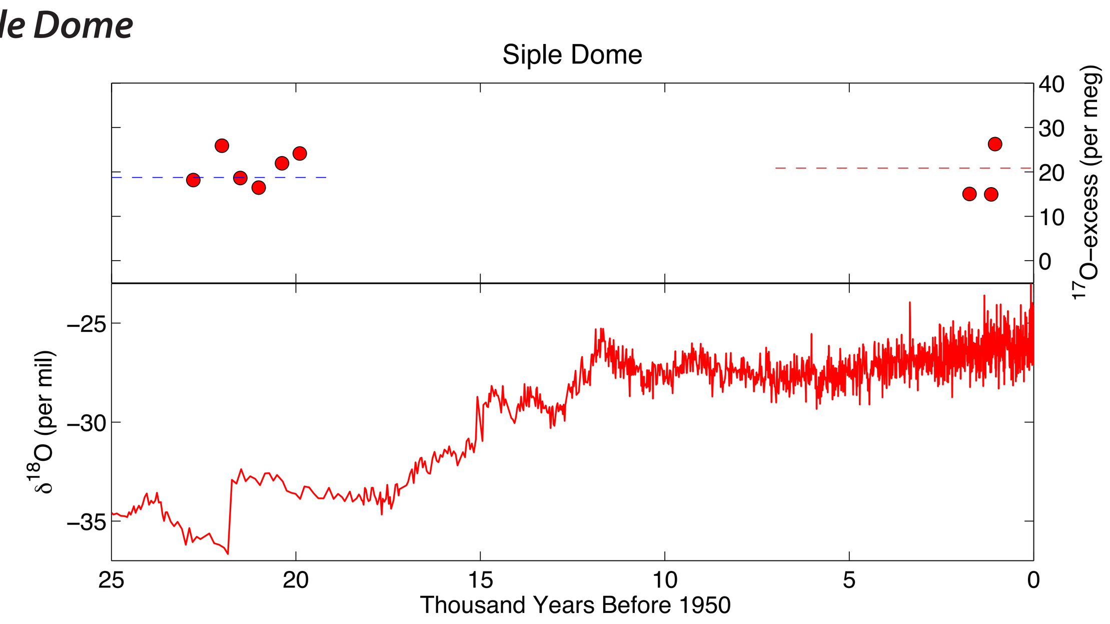

Figure 2. Timeseries of $^{17}O_{excess\,VSMOW\text{-}SLAP}$ (top) and $\delta^{18}O$ (bottom) of the Siple Dome (SD) ice core record from 25ka to 0ka. The glacial (23-19ka) mean $^{17}O_{excess}$ of 19 per meg is not significantly different from the Late Holocene (2-1ka) mean $^{17}O_{excess}$ of 21 per meg. These $^{17}O_{excess}$ results from a coastal ice core site suggest that lower elevation regions may be less sensitive to supersaturation effects on $^{17}O_{excess}$ variations.

Taylor Dome

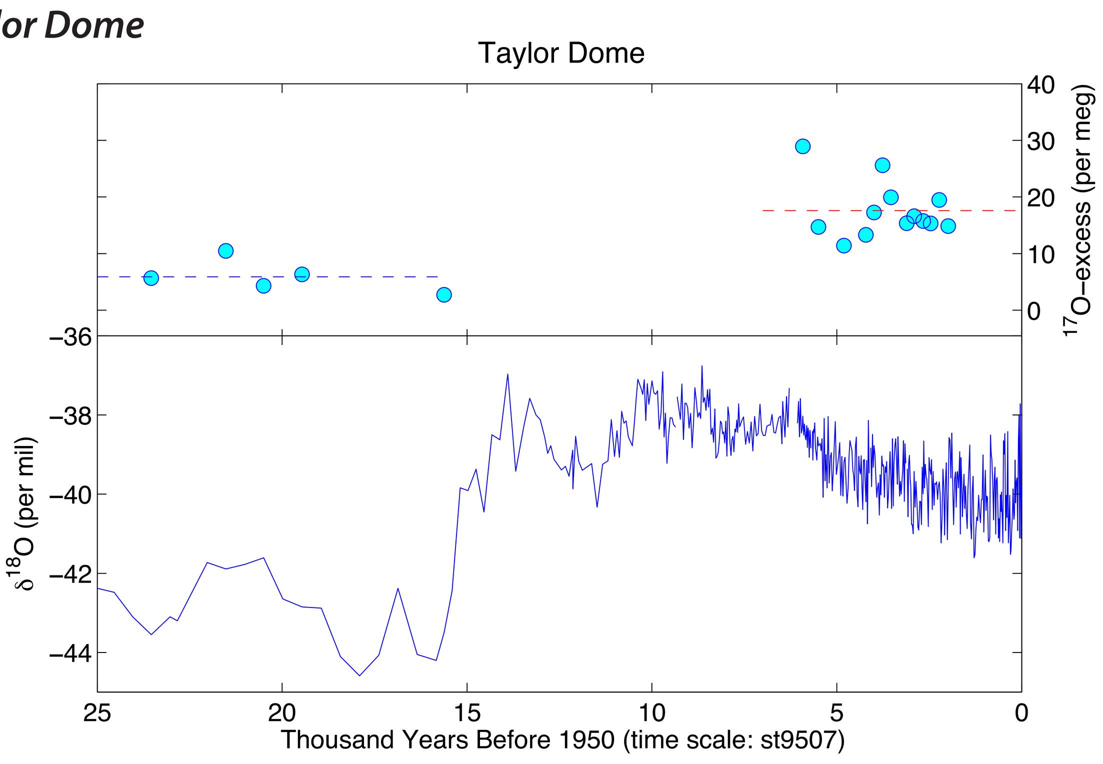

Figure 3. Timeseries of $^{17}O_{excess\,VSMOW\text{-}SLAP}$ (top) and $\delta^{18}O$ (bottom) of the Taylor Dome (TD) ice core record from 25ka to 0ka. The glacial (23-15.5ka) to mid-Holocene (6-2ka) mean $^{17}O_{excess}$ shows a significant (p<0.04) increase of 12 per meg. The TD $\delta^{18}O$ demonstrates a later and more abrupt deglacial warming. The $^{17}O_{excess}$ increase differs from those results found at Talos (Winkler, 2011) that showed no signficant G-IG change.

WD deglacial $^{17}O_{excess}$ magnitude similar to Vostok

At WD the glacial-interglacial change in $^{17}O_{excess}$ is 21 per meg, slightly larger than at Vostok. Although it has been suggested that the glacial-interglacial $^{17}O_{excess}$ change at Vostok may reflect input from high-$^{17}O_{excess}$ water vapor with a stratospheric source, the WAIS Divide results suggest that that is unlikely.

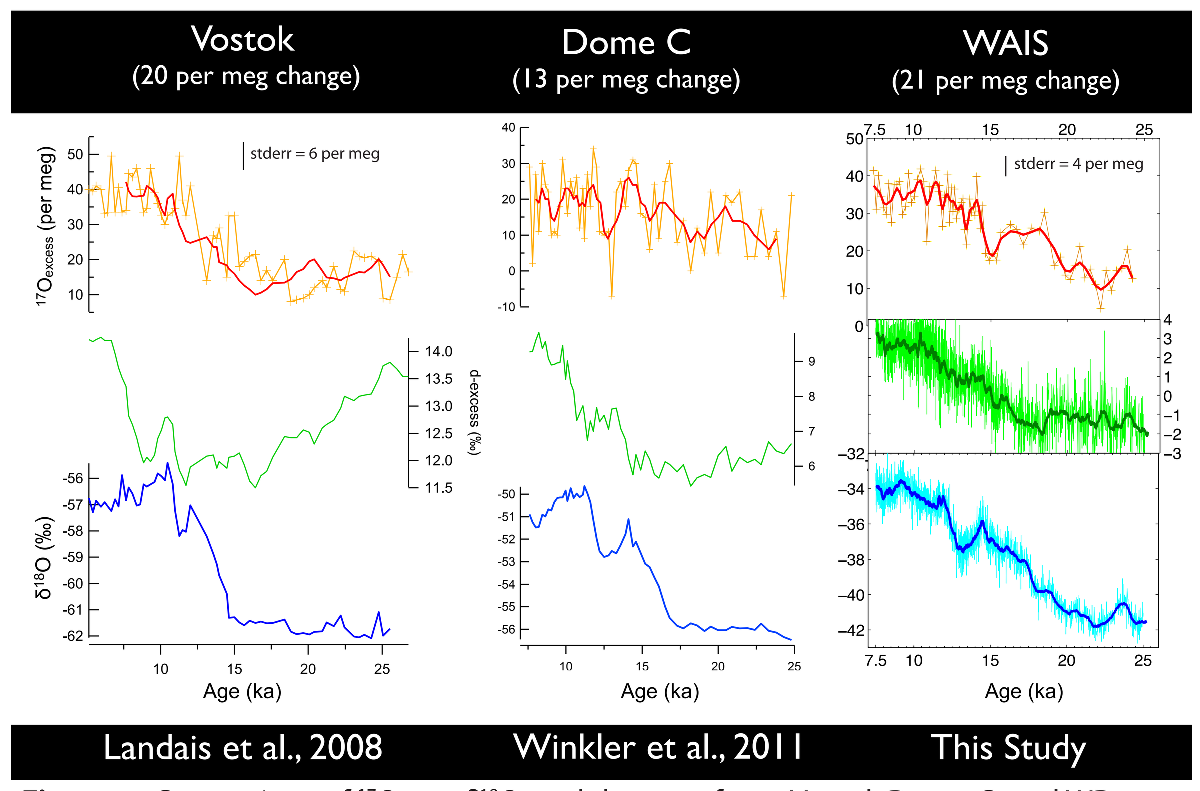

Figure 4. Comparison of $^{17}O_{excess}$, $\delta^{18}O$, and d-excess from Vostok Dome C, and WD

GCM Modeling of $^{17}O_{excess}$

Spatial Gradient

We have added $^{17}O_{excess}$ to the isotope modules of two atmospheric general circulation models: CCSM CAM3 and ECHAM4.6. Both models can qualitatively reproduce the observed spatial distribution of modern $^{17}O_{excess}$ in Antarctic precipitation.

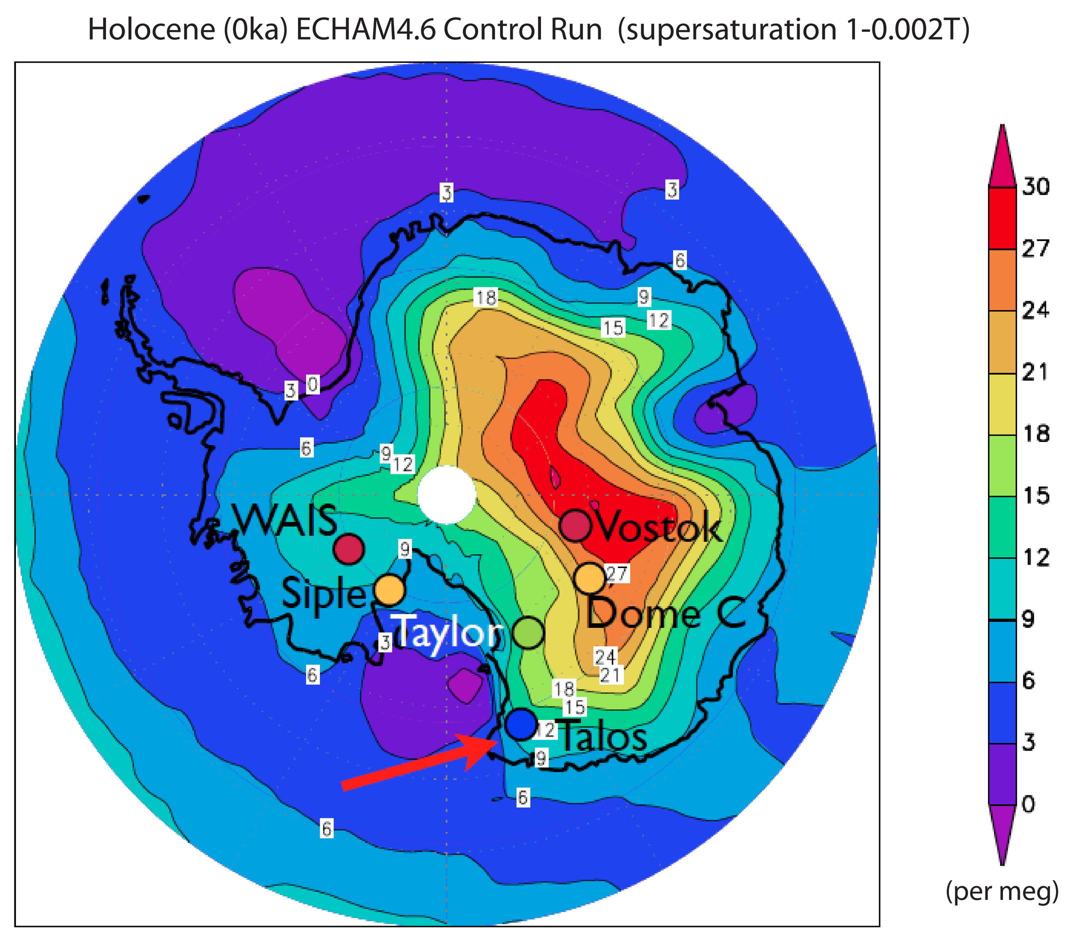

Figure 5. Colored dots indicate measured $^{17}O_{excess}$ from ice core records during the more recent Holocene (6-3ka). The model captures the spatial gradient of $^{17}O_{excess}$, particularly the low values near Talos, most likely due to the presence of the Ross Sea polynya, low sea ice conc. and high normalized relative humidity. West Antarctica $^{17}O_{excess}$ is underestimated, the reason most likely for this is lower topographic resolution in the model.

Factors Controlling $^{17}O_{excess}$

Supersaturation effects between Glacial and Interglacial

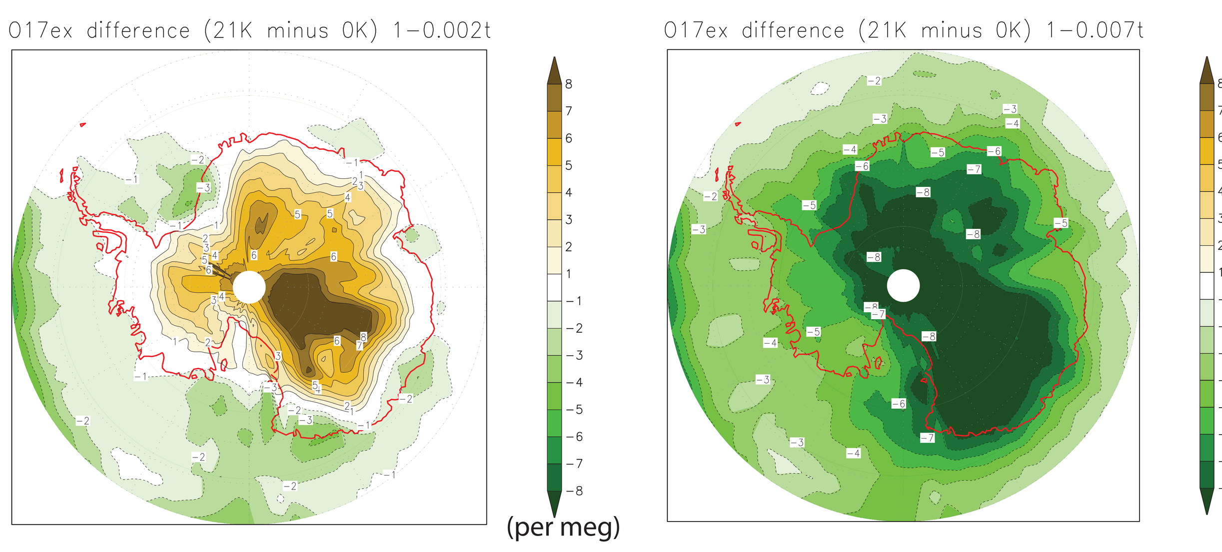

Figure 6. GCM experiments using ECHAM4.6 comparing the effects of different supersaturation values (1-.002T, 1-0.004T, 1-0.007T) between the LGM (21ka) and pre-industrial (0ka). Note that when using modern day supersaturation values the $^{17}O_{excess}$ increases during the glacial, instead a higher supersaturation is necessary to reproduce the low LGM values.

An important factor controlling $^{17}O_{excess}$ is changes in the supersaturation of water vapor over ice under glacial vs. interglacial conditions. Depending on the supersaturation level, kinetic fractionation during snow formation at WAIS could explain part of the signal (~10 per meg), and these effects apply even more strongly at Vostok, due to the colder temperatures and higher elevation of EAIS.

Sea Ice Concentration and Extent

$^{17}O_{excess}$ difference (ctrl-50% sea ice conc.)

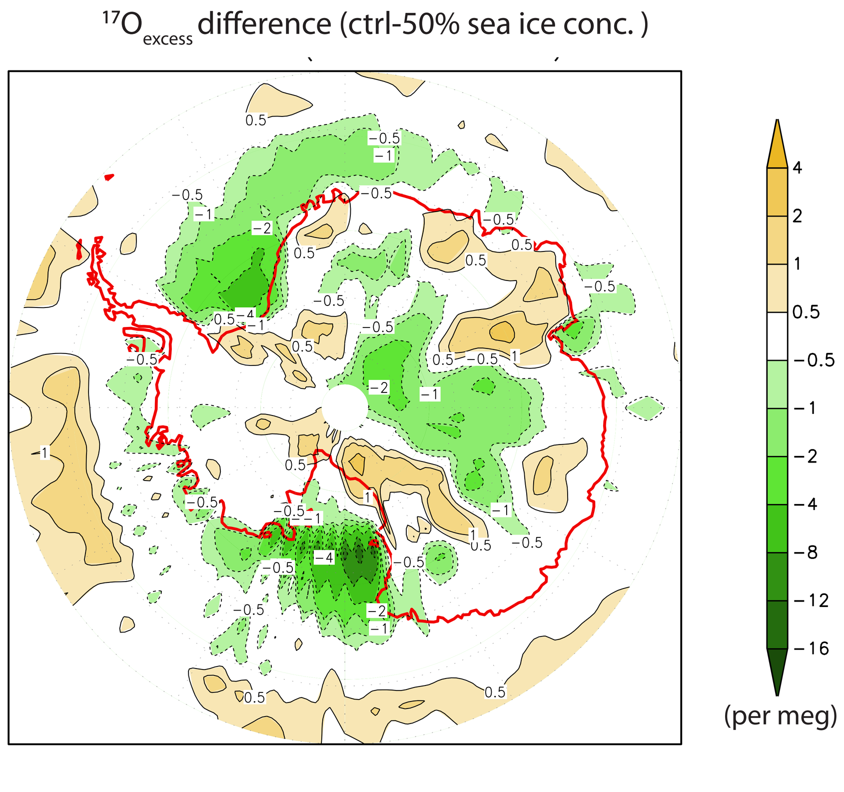

Figure 7. Difference between present day climatological sea ice concentration (control = 100% conc.) and a 50% reduction in annual mean sea ice concentration. In areas with decreased sea ice concentration, $^{17}O_{excess}$ in precipitation increases (more positive), with the largest increases in $^{17}O_{excess}$ occuring in coastal areas of large sea ice production. The largest $^{17}O_{excess}$ increases occur in (JJA-not shown).

Sea Ice Concentration and Extent cont.

d-excess difference (ctrl-50% sea ice conc.)

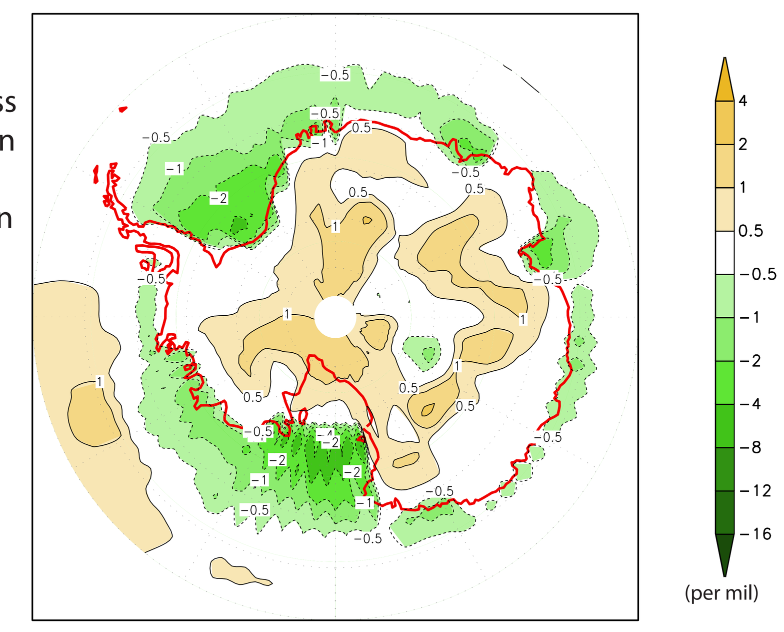

Figure 8. Same as in Figure 7. except for d-excess. Note that d-excess increases (less negative) in coastal regions while it decreases (less positive) in the interior. Noone and Simmonds (2004) obtain similar results, where the d-excess coastal increase is partly attributed to the increased presence of open water.

Other Potential Influences on $^{17}O_{excess}$

Moisture Source Origin & Seasonality: Future work?

Back trajectory results from Sodemann and Stohl (2009):
- Higher wintertime precipitation than summertime. Does this result in a seasonal $^{17}O_{excess}$ bias?
- Winter precipitation dominated by more local moisture sources; further investigate how sea ice concentration and extent influence $^{17}O_{excess}$?
- Moisture sources for WD & Siple originate predominately in the (45-55˚S) latitude, vs. more lower latitude sources for EAIS (40-50˚S).

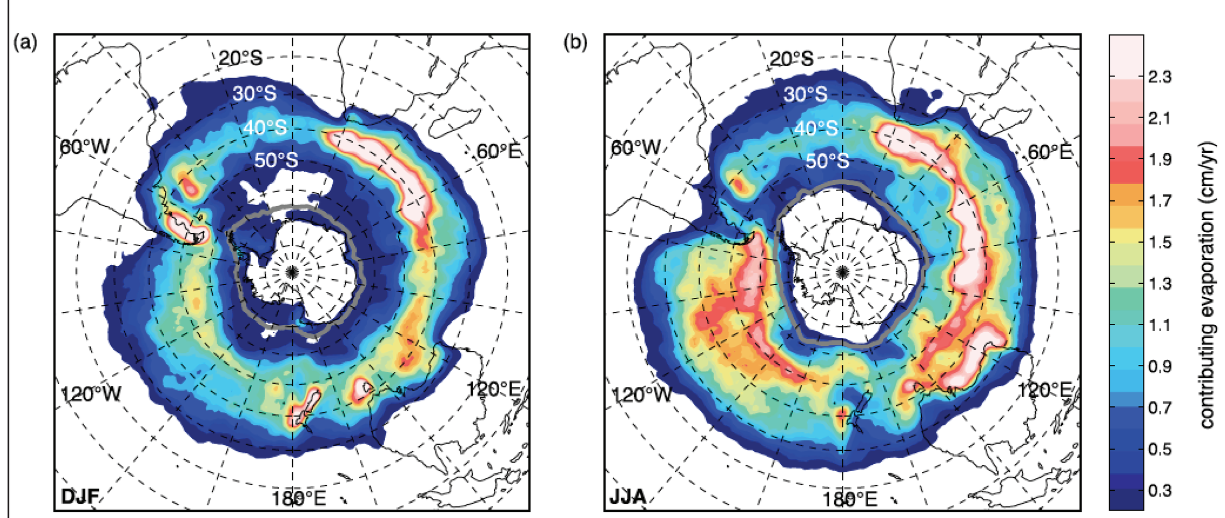

Figure 9. Seasonal mean moisture source regions for Antarctica during (a) summer (DJF) and (b) winter (JJA). Grey line denotes the seasonal mean sea ice boundary. Adapted from Sodemann and Stohl, 2009.

Conclusions

- WD $^{17}O_{excess}$ is ~20 per meg lower during the LGM, comparable to Vostok
- The coastal, low elevation Siple Dome ice core site shows little change in LGM-Holocene $^{17}O_{excess}$, as do modeling results, suggesting that supersaturation effects may only efffect interior sites.
- Simulation of glacial-interglacial changes in ECHAM4.6 realistically captures the differences in magnitude of the glacial/interglacial changes in $^{17}O_{excess}$ between different ice core sites but only under particular parameterizations of supersaturation.
- Our results suggest that the low $^{17}O_{excess}$ values found at Talos Dome and Siple Dome may reflect their proximity to local moisture sources (e.g. from sea ice leads and polynyas) where evaporation into cold air increases the boundary layer humidity, lowering $^{17}O_{excess}$.

Future H_2O $^{17}O_{excess}$ measurements - Laser based

Our lab (IsoLab, University of Washington) in collaboration with Picarro Instruments (Santa Clara, CA) and the Centre for Ice and Climate (Neils Bohr Institute, Copenhagen) have been testing a prototype Picarro cavity-ringdown spectrometer (CRDS). Using a custom vaporizer, we have been introducing continuous water vapor for initial stability testing.

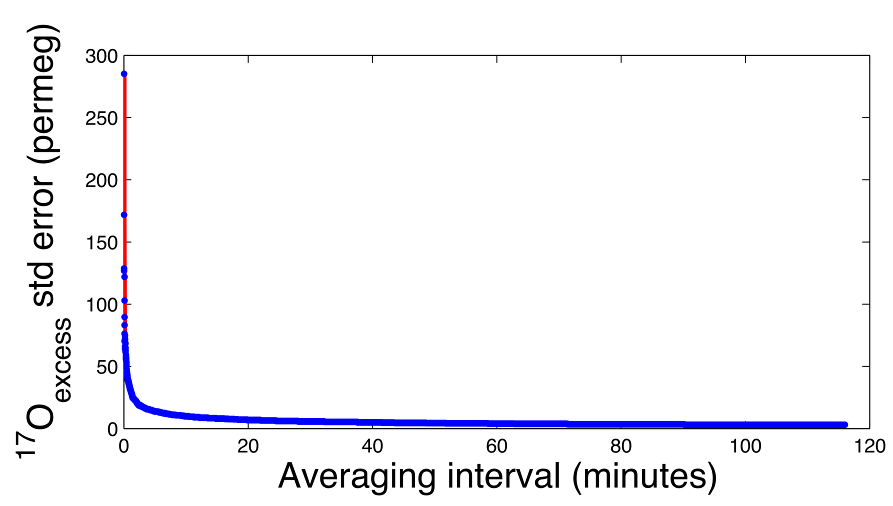

Figure 10. A subset of a 24 hour measurement of an in-house reference water showing 17Oexcess standard error and averaging interval (mins) achieving ~4 per meg precision in ~60 mins

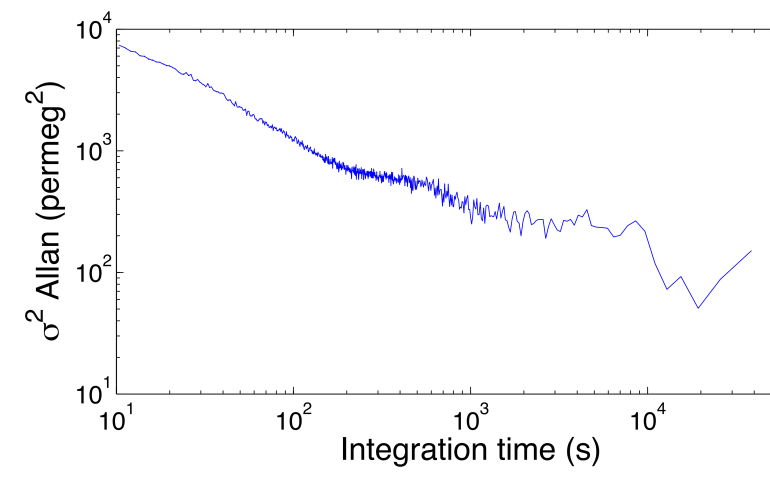

Figure 11. Allan variance for $^{17}O_{excess}$ for same 24 hour measurement as in Figure 10.

References

A. Landais, E. Barkan, B. Luz, Record of $\delta^{18}O$ and $^{17}O_{excess}$ in ice from Vostok Antarctica during the last 150,000 years. *Geophysical Research Letters* 35, L02709 (2008).
D. Noone, I. Simmonds, Sea ice control of water isotope transport to Antarctica and implications for ice core interpretation. *Journal of Geophysical Research* 109, D07105 (May 14, 2004).
H. Sodemann, A. Stohl, Asymmetries in the moisture origin of Antarctic precipitation. *Geophysical Research Letters* 36, L22803 (Nov 20, 2009).
R. Winkler, A. Landais, H. Sodemann, Deglaciation records of $^{17}O_{excess}$ in East Antarctica: reliable reconstruction of oceanic relative humidity from coastal sites. *Climate of the Past*, (2011).